GEOPHYSICAL RESEARCH LETTERS, VOL. 29, NO. 9, 1312, 10.1029/2001GL013544, 2002

Subsidence monitoring using SAR interferometry: Reduction of the atmospheric effects using stochastic filtering

Michele Crosetto
Institute of Geomatics, Barcelona, Spain

Carl Christian Tscherning
Department of Geophysics, University of Copenhagen, Copenhagen, Denmark

Bruno Crippa
Department of Earth Sciences, University of Milan, Milan, Italy

Manuel Castillo
Institut Cartogràfic de Catalunya, Barcelona, Spain

Received 31 May 2001; revised 5 October 2001; accepted 29 October 2001; published 9 May 2002.

[1] The atmospheric effects represent one of the major limits of SAR interferometry as a quantitative technique to monitor subsidences. In this work, which focuses on subsidences of small spatial extent, a procedure to reduce these effects is described. The atmospheric component of the interferometric phase is estimated adopting a filtering and prediction procedure, which exploits the phase over stable areas identified in the vicinity of the analysed subsidence area. The procedure was validated on a suitable test site located in North-eastern Spain. Furthermore, it was employed in the study of a small-scale subsidence, where the interferometric results were validated using precise geodetic observations. *INDEX TERMS:* 1204 Geodesy and Gravity: Control surveys; 0933 Exploration Geophysics: Remote sensing

1. Introduction

[2] The quantitative monitoring of subsidences, which may provide a valuable support to the decision makers, often needs to be characterised by high quality standards, like those achieved by the geodetic techniques. The differential interferometric SAR (D-InSAR) technique has demonstrated its capability to measure subsidences [*Carnec et al.*, 1996; *Amelung et al.*, 1999; *Tesauro et al.*, 2000]. However, some of the published investigations rather focus on a qualitative use of the InSAR results, and in order to achieve the above standards different aspects of the technique have to be improved. This work, which concerns subsidences of small spatial extent, is focused on the atmospheric effects, one of the major limits of InSAR as a quantitative monitoring technique. To mitigate the quality degradation caused by these effects, redundant observations, i.e. more than two SAR images, are often used [*Massonnet and Feigl*, 1995; *Ferretti et al.*, 2001]. In this paper we propose a new procedure to reduce the atmospheric effects, which may be effective even with a single image pair. Using a priori available information, it is often possible to identify stable areas in the vicinity of the deformation area under analysis. The stable areas are used to perform a quantitative analysis of the atmospheric effects on a given interferogram. Furthermore, adopting a suitable filtering and prediction technique, they are employed to estimate the atmospheric component of the InSAR phase and to predict it over the deformation area, hence improving the quality of the generated deformation maps. The next section provides a brief description of the procedure. Two experiments, located in Catalonia (North-eastern Spain), are then discussed. In the first one, the technique is validated over a stable test area, giving a quantitative assessment of the reduction of the atmospheric effects. In the second one, an application to a small-scale urban subsidence, where geodetic observations are used to validate the interferometric results, is described.

0094-8276/02/2001GL013544

2. The Filtering and Prediction Procedure

[3] The unwrapped differential phase Φ, computed with the digital elevation model (DEM) elimination method [*Massonnet et al.*, 1994], consists of the following components:

$$\Phi = \Phi_M + \Phi_A + \Phi_T + \Phi_N \quad (1)$$

where Φ_M is the terrain movement component, Φ_A the atmospheric contribution, Φ_T the residual topography component due to DEM errors, and Φ_N is the decorrelation noise [*Ferretti et al.*, 2001]. The systematic component due to orbital errors is not included in (1) because it is removed using a suitable InSAR geometry refinement based on ground control points. The atmospheric effects are due to microwave propagation heterogeneities, which result in a spatial variation of Φ_A [*Hanssen*, 2001]. Considering the stable areas, where Φ_M is naught, it is possible to evaluate the influence of atmospheric heterogeneities on the interferogram at hand. In case the atmospheric delay is constant over the interferogram, the spatial variation of Φ is due to Φ_T and Φ_N, which can be considered spatially decorrelated (hereafter they are referred to as the noise). As far as Φ_T is concerned, this assumption holds for high quality DEMs, e.g. the high resolution photogrammetric DEMs, while it does not hold for InSAR DEMs, potentially affected by atmospheric effects. In the presence of atmospheric heterogeneities, Φ_A varies over the interferogram and represents the correlated part of Φ (Φ_A is referred to as the signal). The contribution of Φ_A can be assessed by analysing the spatial autocorrelation of Φ. The analysis is based on the autocovariance function (AF), whose characteristic parameters are the variance of the signal σ_S^2 and the correlation length L_C. In the literature, the atmospheric effects are usually described through the power spectrum [*Hanssen*, 1998]. The AF, whose information content is equivalent to that of the power spectrum, is estimated in the image space with a procedure which

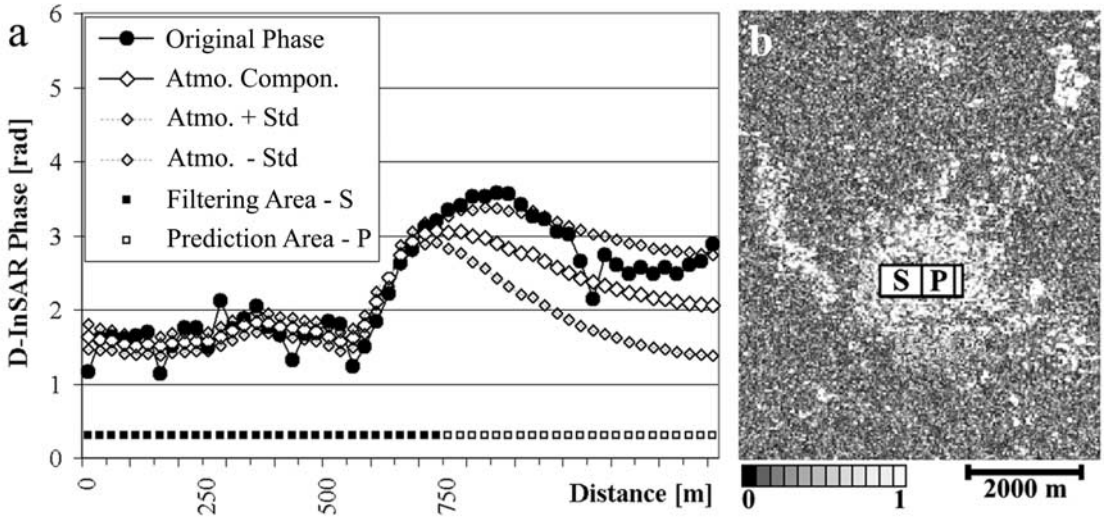

Figure 1. Validation of the procedure over the Manresa area. (a) Profile of I1: Original phase Φ, filtered (Φ_{Af}, left) and predicted Φ_A (Φ_{Ap}, right), with the associated confidence bands (signal ± standard deviation, Std). (b) Coherence sub-image (6 by 7.5 km) of the test side: location of the filtering and prediction areas (*S* and *P*). The narrow stable area, which is used in the Case 2 (Table 1), is located on the right side of *P*. The urban areas correspond to the lighter grey values.

works with both regular and sparse grids [*Crosetto et al.*, 2001]. An interferogram weakly affected by atmospheric effects will be characterised by a nearly zero value of σ_S^2 and L_C, while in the presence of atmospheric heterogeneities the two parameters will be significantly different from zero. This property can be used to classify reliable and potentially degraded interferograms. Taking advantage of the above correlation characteristics, it is possible to extract the signal over the stable areas and to predict it over the subsidence area. The predicted signal Φ_{Ap} is subtracted from the phase Φ, hence reducing the atmospheric effects (after the correction a residual component, $\Phi_A - \Phi_{Ap}$, will remain). This step is performed using the method of least squares collocation, a flexible stochastic filtering technique widely employed in geodesy [*Moritz*, 1978; *Dermanis*, 1984]. Assuming Φ over the stable areas to be a realization of a 2D stationary stochastic process, the collocation method separates the signal Φ_A from the noise (filtering), using the AF of the process, which is estimated from the original data Φ. Besides filtering, the collocation method can be used to estimate the signal over locations not covered by the original data (prediction). The proposed procedure offers two cardinal advantages. Firstly, it fully exploits all the available information on the atmospheric effects that are suitably described by the AF. Secondly, it provides an adaptative filtering, which is only driven by the AF, without requiring any explicit modelling of Φ_A: it is by far more flexible than any classical interpolation technique, like polynomials, etc. It is worth to stress two further characteristics of the collocation method. It predicts Φ_{Ap} values that tend to the mean of Φ over the stable areas when the prediction variance σ_p^2 increases (σ_p^2 grows with the distance to the nearest stable area). This property guarantees that the predicted signal does not diverge over any far prediction location. The same cannot usually be guaranteed by model-based extrapolation procedures. Finally, the technique provides the filtered and predicted signals with their associated variance-covariance matrices, thus fully describing the stochastic features of the output.

3. Validation of the Procedure

[4] The procedure was tested using four independent ERS-1/2 interferograms. A stable area, located in the city of Manresa (Catalonia, North-eastern Spain), was chosen as a test site. The conditions of a small-scale subsidence were simulated. In each interferogram, two adjacent areas were arbitrarily chosen: a 750 by 600 m filtering area, playing the role of stable area, and a 600 by 600 m prediction area, acting as subsidence area. The interferogram pixel footprint is about 20 by 24 m (a six look azimuth compression was performed). The whole test site is actually a stable area, where Φ_M is naught, and this characteristic was exploited in the validation. This was based on the comparison of the original phase Φ with the corrected phase, $\Phi - \Phi_{Ac}$, where Φ_{Ac} is either the filtered Φ_A, Φ_{Af}, or the predicted one, Φ_{Ap}. Ideally, both Φ_{Af} and Φ_{Ap} should equal Φ_A and the corrected phase $\Phi - \Phi_{Ac}$ should be a zero mean noise. In reality, possible filtering and prediction errors will cause a spatial correlation and a bias in the corrected phase. The validation was based on the comparison of the AFs and biases of Φ and $\Phi - \Phi_{Ac}$. The four interferograms (I) come from seven ERS-1/2 images, acquired between June 1995 and July 1999, that have the following perpendicular baselines: 6 m for I1 and I2, 8 m and 107 m for I3 and I4, respectively. Despite the large time spans (1364, 981, 455 and 1365 days), they have a quite high coherence over the test site: the four mean coherence values are above 0.4. The differential interferograms were computed using a 15 m DEM, generated at the Institut Cartogràfic de Catalunya (ICC) as a by-product of 1:5000 maps, and characterized by a RMS error of 1–2 m. The filtering and prediction were performed on the unwrapped phases using the GRAVSOFT package [*Tscherning et al.*, 1994]. For each interferogram, the corresponding AF was estimated over a 3 by 2 km stable area, excluding the 600 by 600 m prediction area. I3, the interferogram less affected by atmospheric effects, has L_C of 40 m, while the others have L_C of about 200 m. A profile of I1 is shown in Figure 1, where Φ_{Af} and Φ_{Ap} are superposed to the original phase Φ. In the filtering area (left side) the signal Φ_{Af} is well separated from the noise, while in the prediction area there are some discrepancies between Φ and Φ_{Ap}. Note that this is well reflected by the corresponding confidence bands. The statistics on Φ and $\Phi - \Phi_{Af}$, computed using four filtering windows, confirmed that the correlated part of Φ, Φ_{Af}, was accurately estimated: Φ is spatially correlated in all interferograms, while $\Phi - \Phi_{Af}$ basically consists of a decorrelated noise (L_C and σ_S^2/σ_T^2, where σ_T^2 is the variance of Φ, are both zero).

Table 1. Validation of the collocation prediction over four interferograms

	Original phase			Corrected phase: Case 1			Corrected phase: Case 2		
	Mean [rad]	σ_S^2/σ_T^2 [%]	L_C [m]	Mean [rad]	σ_S^2/σ_T^2 [%]	L_C [m]	Mean [rad]	σ_S^2/σ_T^2 [%]	L_C [m]
I1	0.84	47.2	114.1	0.35	20.6	66.7	0.21	15.5	56.0
I2	1.07	50.8	51.5	0.56	55.4	61.3	0.01	34.1	30.6
I3	0.22	24.8	39.9	0.22	24.7	39.8	0.14	24.1	39.3
I4	0.81	47.6	108.8	0.83	45.1	94.0	0.16	30.2	40.1

Statistics over a 600 by 600 m prediction window (target) of the original phase Φ and the corrected one, $\Phi - \Phi_{Ap}$, computed in two different scenarios (see Figure 1): a 750 by 600 m stable area adjacent to the target (Case 1), and two stable areas (750 by 600 m and 100 by 600 m, respectively) that include the target (Case 2). The more favourable conditions of Case 2 result in a better prediction: the mean of the corrected phase (bias), σ_S^2/σ_T^2 and L_C are sensibly smaller than those of Case 1.

[5] In Table 1 are reported the statistics concerning the prediction area. The mean of the original phase Φ represents the bias caused by Φ_A, while the mean of $\Phi - \Phi_{Ap}$ measures the residual bias due to the prediction error, $\Phi_A - \Phi_{Ap}$. In the Case 1, the bias reduction only regards I1 and I2, while in the Case 2 it is stronger and concerns all pairs. Likewise occurs for the reduction of the spatial correlation. These results indicate that over small-scale areas the proposed procedure can significantly reduce the atmospheric effects. It is worth to emphasise that the procedure can be employed with any interferogram: if there are atmospheric effects, they can be reduced; otherwise the atmospheric correction has no consequence. This occurs, for instance, for I3, which is affected by weak atmospheric effects, see Table 1. This property is automatically driven by the AF, which is estimated on each interferogram. In fact, if there are no atmospheric effects, the correlation will be negligible and the collocation method will predict values Φ_{Ap} that tend to the mean of Φ over the stable areas. That is, the atmospheric correction will have no consequence. The procedure suffers for its intrinsic limitation related to the non-stationarity of the analysed signal, which practically confines its use to the vicinity of the stable areas. This can be proved considering smaller prediction areas near the stable area. Taking the Case 1 scenario with a maximum prediction distance that equals L_C (i.e. the first 200 m for I1, I2 and I4, instead of 600 m), there is a remarkable reduction of the prediction error: after phase correction, both L_C and σ_S^2/σ_T^2 are reduced to values that are less than 30% of those reported in Table 1.

4. Application to a Small-Scale Urban Subsidence

[6] The procedure was employed in the analysis of an urban subsidence of small spatial extent, located in the village of Sallent (Catalonia, North-eastern Spain). A portion of the village, which lies on an old pottassic salt mine, is subjected to subsidence. Since July 1997 this area is monthly monitored using high precision geodetic levelling. An assessment of the subsidence was based on the four D-InSAR pairs mentioned in the previous section. For each pair, a subsidence map based on a classical D-InSAR procedure, and its corresponding atmospherically corrected map were derived. In the Sallent area, an accurate map of the old salt mine is available, see the dark area in Figure 2b: a 500 by 750 m stable area was chosen outside the mine border. Over the stable area, I1 and I4 have a quite high correlation, indicating the presence of atmospheric effects: the L_C and σ_S^2/σ_T^2 values are similar to those reported in Table 1 (third and fourth columns). On the contrary, I2 and I3 are characterized by a very weak spatial correlation, i.e. they are affected by negligible atmospheric effects. The four pairs were separately processed. The phase unwrapping was performed taking the reference phase on the old centre of Sallent, a stable area that is located about 800 m from the

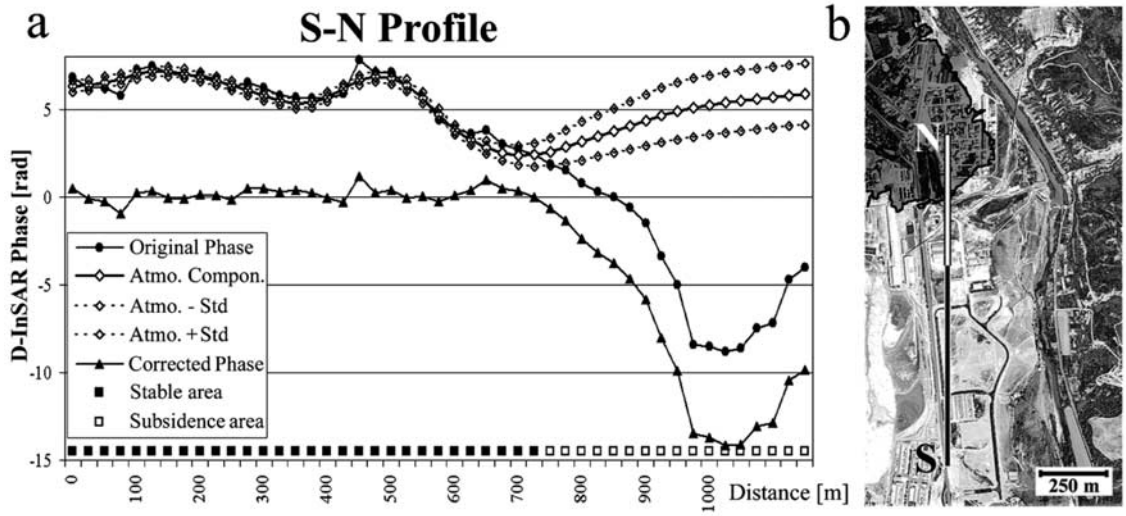

Figure 2. Reduction of the atmospheric effects over the urban subsidence of Sallent. (a) Profile over the original phase Φ, filtered (left) and predicted (right) atmospheric component with the associated confidence bands (estimated atmosphere ± standard deviation, Std), and corrected phase. (b) Orthoimage of Sallent: the subsidence area is in the upper-left part (the old mining area corresponds to the dark field), while the stable area is in the bottom half part of the image.

subsidence centre. The four maps derived with the classical D-InSAR procedure fit quite well with the reference data: they both include an ellipse-shaped area of deformation, with length of axes of about 120 m and 200 m. The D-InSAR and geodetic measures refer to time intervals that do not overlap: from 1995 to 1999 for the D-InSAR data and from July 1997 to May 2001 for the geodetic measures. The latter ones clearly display a linear behaviour of the subsidence at hand. In order to perform the validation, the geodetic data were linearly extrapolated to 1995. The maximum deformations measured with I2 and I3 equal 5.4 and 2.6 cm, while the corresponding reference values are 5.7 and 2.7 cm, respectively. These results confirm the good phase quality of I2 and I3 in the Sallent area. The same cannot be said for I1 and I4, whose maximum deformations, 4.2 and 5 cm, significantly differ from the corresponding reference value (7.9 cm). The atmospheric effects were considered as a possible cause of these important differences. The reduction of these effects was based on the 500 by 750 m stable area, which is located about 300 m from the centre of the subsidence. The autocovariance functions used in the collocation prediction have L_C of 200 m for both I1 and I4. The results obtained for I1 are illustrated in Figure 2. The original phase Φ is affected by a strong atmospheric component, which in the stable area shows a strong spatial variation. Over this area the corrected phase $\Phi_A - \Phi_{Af}$ consists of a zero-mean noise, indicating that Φ_A was properly removed. Over the maximum of the subsidence, the estimated Φ_{Ap} equals 5.4 rad (2.6 cm of in terms of vertical subsidence), with a standard deviation of 1.7 rad. For I4, Φ_{Ap} equals 3.7 rad, with a standard deviation of 0.93 rad. After atmospheric correction, the maximum deformation equals 6.8 cm, for both I1 and I4. This represents a remarkable improvement with respect to the original results. It must be noted that the coincidence of the two values has to be considered fortuitous. It is interesting to consider the standard deviation associated with the D-InSAR observations: 0.6 and 0.9 cm for I4 and I1 respectively. These values include two contributions: the standard deviation of the atmospheric correction, estimated by collocation (0.53 cm for I4), and that of the original phase (0.3 cm for I4) computed as a function of the coherence [*Hanssen*, 2001], which around the subsidence centre is about 0.4. If multiple D-InSAR observations are available, the standard deviation provides a fundamental quality measure to drive the data fusion procedure (weighting of the observations). Taking into account the standard deviations of the observations, assumed to be normally distributed, a simple significance test can be carried out: the difference between the D-InSAR observations and the reference measure (1.1 cm in both cases) cannot be considered statistically significant, for both I1 and I4, even choosing a confidence level as high as 10%.

5. Conclusions

[7] A procedure to reduce the atmospheric effects in D-InSAR observations of small-scale subsidences has been proposed. It takes advantage of the phase over stable areas, located in the vicinity of the subsidence under analysis. It involves the filtering and the prediction of the atmospheric component, which is performed using the method of least squares collocation, a flexible stochastic filtering technique. The procedure considers the stable areas in a deterministic way: a possible subsidence inside the supposed stable areas may prejudice the results. This could be avoided in a straightforward extension, weighting the different stable areas according to their degree of reliability. The procedure may be used on both regular and sparse grids. In the latter case, appropriate unwrapping techniques are needed [*Costantini and Rosen*, 1999]. The procedure has been validated over a stable urban area located in North-eastern Spain: the atmospheric effects have been significantly reduced in all considered cases. The reduction mainly depends on the geometric conditions (Case 1 vs. Case 2) and on the prediction distance. The non-stationarity of the atmospheric component represents a major limit of the procedure. The effectiveness of the procedure has been confirmed in the analysis of a small-scale urban subsidence: by removing the atmospheric effects, a remarkable accuracy improvement has been achieved. The reliability of the deformation maps could be improved using multiple interferograms, firstly applying the above procedure on each interferogram, and then performing the data fusion.

[8] **Acknowledgments.** This work has been partially funded by the Italian COFIN 2000, protocol MM04158184, "Active deformation at the northern boundary of Adria".

References

Amelung, F., D. L. Galloway, J. W. Bell, H. A. Zebker, and R. J. Laczniak, Sensing the ups and downs of Las Vegas: InSAR reveals structural control of land subsidence and aquifer-system deformation, *Geology*, *27*(6), 483–486, 1999.

Carnec, C., D., Massonnet, and C. King, Two examples of the use of SAR interferometry on displacement fields of small spatial extent, *Geophys. Res. Lett.*, *23*(24), 3579–3582, 1996.

Costantini, M., and P. Rosen, A generalized phase unwrapping approach for sparse data, *Proc. Int. Geosci. Remote Sensing Symp.*, Hamburg, Germany, June 28–July 2 1999, pp. 267–269.

Crosetto, M., J. A. Moreno Ruiz, and B. Crippa, Uncertainty propagation in models driven by remotely sensed data, *Remote Sensing of Environment*, *76*(3), 373–385, 2001.

Dermanis, A., Kriging and collocation: A comparison, *Manuscripta Geodaetica*, *9*(3), 159–167, 1984.

Ferretti, A., C. Prati, and F. Rocca, Permanent scatterers in SAR interferometry, *IEEE T. Geosci. Remote*, *39*(1), 8–20, 2001.

Hanssen, R., Atmospheric heterogeneities in ERS tandem SAR interferometry, Delft University Press, Delft, The Netherlands, 1998.

Hanssen, R., Radar interferometry, Kluwer Academic Publishers, Dordrecht, The Netherlands, 2001.

Massonnet, D., and K. L. Feigl, Discrimination of geophysical phenomena in satellite radar interferograms, *Geophys. Res. Lett.*, *22*(12), 1537–1540, 1995.

Massonnet, D., K. L. Feigl, M. Rossi, and F. Adragna, Radar interferometric mapping of deformation in the year after the Landers earthquake, *Nature*, *369*, 227–230, 1994.

Moritz, H., Least-squares collocation, *Rev. Geophys. Space Phys.*, *16*, 421–430, 1978.

Tesauro, M., P. Berardino, R. Lanari, E. Sansosti, G. Fornaro, and G. Franceschetti, Urban subsidence inside the city of Napoli (Italy) observed by satellite radar interferometry, *Geophys. Res. Lett.*, *27*(13), 1961–1964, 2000.

Tscherning, C. C., P. Knudsen, and R. Forsberg, Description of the GRAVSOFT package, Geophysical Institute, University of Copenhagen, Technical Report, 1994.

M. Crosetto, Institute of Geomatics, Parc de Montjuïc, 08038 Barcelona, Spain. (michele.crosetto@ideg.es)

C. C. Tscherning, Department of Geophysics, University of Copenhagen, Juliane Maries Vej 30, 2100 Copenhagen, Denmark. (cct@gfy.ku.dk)

B. Crippa, Department of Earth Sciences, University of Milan, via Cicognara 7, 20129 Milan, Italy. (bruno.crippa@unimi.it)

M. Castillo, Institut Cartogràfic de Catalunya, Parc de Montjuïc, 08038 Barcelona, Spain. (manuelc@icc.es)